JOURNAL OF THERMOPHYSICS AND HEAT TRANSFER
Vol. 8, No. 2, April–June 1994

Two-Slab Model of Plasma Mediated Laser Coupling to Surfaces

Guy Weyl*
Physical Sciences Inc., Andover, Massachusetts 01810

The interaction of a laser beam with a surface in vacuum is modeled when the vapor products emanating from the surface have formed a plasma. The vapor is treated as being composed of two layers: 1) a hot outer layer of plasma that absorbs all the laser radiation and reradiates in the UV and vacuum UV (VUV); and 2) a colder inner layer that absorbs the plasma radiation, thereby shielding the surface from most of the UV and VUV radiation, resulting in reduced vaporization. Results are presented for aluminum and carbon surfaces when the plasma temperature is in the range 2–20 eV, corresponding to laser intensities in the range 10^6–10^{10} W/cm^2.

Nomenclature

A, B = constants in Eq. (9)
$A'B'$ = constants in Eq. (10)
a = speed of sound
C_v = specific heat at constant volume
D_1, D_2, D_3 = constants in Eq. (8)
E = energy per unit mass
F = constant in Eq. (8)
g_j = degeneracy of state j
H_v = heat of vaporization
h = Planck constant
I = intensity
K = constant in Eq. (4)
k = absorption coefficient
k_B = Boltzmann constant
L = slab thickness
l_R = Rosseland mean absorption length
M = mass per unit area
$\dot{M}$ = mass loss rate per unit area
n = number density
R = beam radius
T = temperature, eV
t = time
t_p = pulse duration
x = axial distance
Z = degree of ionization, charge
γ = ratio of specific heats
ε = energy, emissivity
θ_j = temperature, solution of Eq. (5)
λ = wavelength
μ = atomic mass
ν = frequency
ρ = density
ρ_0 = reference density, 1.2×10^{-3} g/cm^3
σ = Stefan-Boltzmann constant

Subscripts

e = for electrons
j = for ion of charge j
s = at the surface
1, 2 = refers to slab I, II

Received April 14, 1992; revision received July 8, 1993; accepted for publication July 13, 1993.

*Principal Research Scientist, 10 New England Business Center; currently Network Physics, 23 Somerset Road, Lexington, MA 02173.

Introduction

WHEN a high-power laser beam irradiates an absorbing surface, the surface will heat up and eventually vaporize. Most vapors are transparent throughout the visible and near infrared. The formation of a vapor will not, therefore, prevent the laser radiation from reaching the surface, or impede further vaporization of the surface so long as the laser wavelength is neither too short ($\lambda > 0.3$ μm) nor too long ($\lambda < 1$ μm). If the vaporization temperature is high enough that the vapor comes off partially ionized, then inverse bremsstrahlung absorption by the electrons may lead to vapor breakdown and plasma formation by cascade ionization,[1,2] or by thermal runaway.[2] The plasma thus formed will be a strong absorber of laser radiation and will shield the surface from the laser beam, thus reducing the vaporization rate. One would expect the vaporization to occur intermittently, the vaporization being turned off when a plasma has been formed and resuming at a later time, once the plasma has become transparent due to axial and lateral expansion.

Basov et al.[3] noted that as the temperature of the plasma increased, its transparency to the laser radiation also increased. The plasma could, therefore, evolve during the laser pulse in such a way as to preserve some laser coupling to the surface. The "self regulating" model that they developed was based on the assumption that the relation $kL = 1$ is always satisfied at short pulse times when $L \ll R$ (one-dimensional regime) or $kR = 1$ at longer times when $L > R$ (three-dimensional regime). In the one-dimensional regime, the axial extent of the plasma was assumed to vary as $L = at$, and they obtained the following scaling laws:

$$\rho \propto t^{-3/8} I^{1/4}, \qquad T \propto t^{1/4} I^{1/2}, \qquad \dot{M} \propto \rho t^{1/2} \propto t^{-1/8} I^{1/2}$$

These scaling laws are not expected to be valid for metallic and semimetallic surfaces such as Al and C at laser intensities $I < 10^{12}$ W/cm^2, since the energy equation of state and the inverse bremsstrahlung k that they used were based on a plasma consisting of electrons and fully stripped ions having a kinetic energy greatly in excess of the ionization energy of the vapor (which was neglected).

Also, the Basov model does not take into account radiation by the plasma which provides another mechanism for continued coupling to the surface. If the plasma were optically thick to its own radiation, then the plasma slab would radiate onto the surface and into space, a power per unit area σT^4. The asymptotic temperature that it would reach would be $T = (I/2\sigma)^{1/4}$ and could not increase as $t^{1/4}$, as predicted by the model.

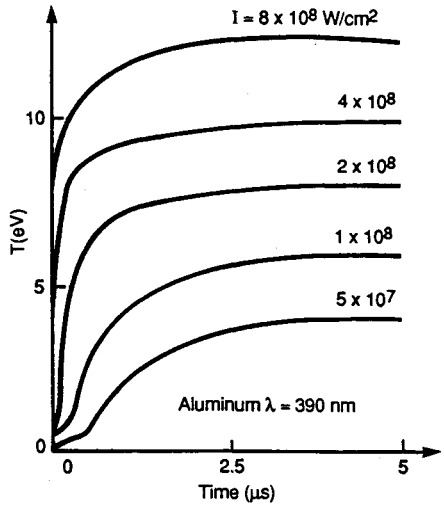

Fig. 1 Maximum plasma temperature vs time, from Ref. 2.

Radiative transport in an aluminum plasma has been included in later studies[4-7] and was found to play a dominant role in the coupling after an absorbing plasma has been formed. We show in Fig. 1 the results of Bergelson and Nemchinov[4] who solved the coupled fluid dynamics and radiative transport in an aluminum plasma in the one-dimensional regime. This figure shows that after an initial transient, corresponding to formation and heating of the plasma, the peak plasma temperature reaches an asymptotic value corresponding to $2\varepsilon\sigma T^4 = I$, where ε increases from 0.16 to 1 as I decreases from 8×10^8 to 5×10^7 W/cm^2. Figure 4 of their paper[4] gives temperature profiles in the vapor which show that, when the absorption length at the laser wavelength is comparable to the mean free path of radiation emitted by the plasma, the temperature profile of the plasma is fairly flat. Adjacent to the surface there is a colder layer of vapor/plasma of integrated mass density $\approx 10^{-4}$ g/cm^2 that shields the surface from the radiation emitted by the hot outer plasma. It is this latter observation which has led us to consider a simplified two-slab model of plasma mediated interaction to describe the interaction of a high-power laser beam with a surface. The two-slab model, as we shall see, should yield reasonably accurate results for laser wavelengths $0.1 < \lambda < 1$ μm over the intensity range considered $10^6 < I < 10^{10}$ W/cm^2.

Description of Model

We assume that, after a transient time Δt, a plasma has been ignited above the surface of a given material and has reached a "steady-state" T. The geometry is shown in Fig. 2a. We have two slabs: one (slab I) of constant mass per unit area near the surface composed of high-density, low-temperature vapor that has come off the surface, and a much higher temperature, low-density slab (slab II) of thickness L which has absorbed the laser radiation and has been heated up by it. Vaporization of the surface occurs due to a trickle through of VUV radiation emitted by slab II that has been transmitted through slab I. Heating of slab I occurs due to absorption of the majority of VUV radiation (I_{vuv}) emitted toward the surface.

Assume that slab II is at constant T and is emitting radiation of magnitude $\varepsilon\sigma T^4$ into vacuum. By symmetry there must also be $\varepsilon\sigma T^4$ emitted toward the surface, as shown in Fig. 2b. A small fraction of this radiation actually reaches the surface, with most of the energy being used up to heat the vapor in slab I to the temperature of slab II. We thus write

$$\varepsilon\sigma T^4 = \dot{M}\left(H_v + \int_{T_s}^{T} C_v\, dt' + \frac{1}{2}a^2\right) \qquad (1)$$

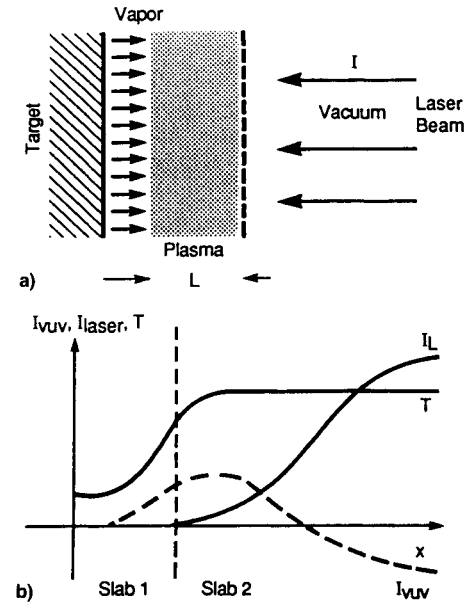

Fig. 2 Model for plasma mediated coupling: a) geometry and b) profiles of I_L, I_{vuv}, and T.

Equation (1) is a steady-state equation which simply states that the mass of and conditions in slab I remain constant in time. By conservation of energy, we must also have

$$M_2 \frac{dE}{dt} + \varepsilon\sigma T^4 + \dot{M}\left(H_v + \int_{T_s}^{T} C_v\, dT' + \frac{1}{2}a^2\right) = I \qquad (2)$$

Equations (1) and (2) are all that are needed to solve the problem if we know the emissivity ε of slab II. ε depends on ρ, T, and L. As a first approximation, one can set T = const and write that $L(t) = at$, and also write $\rho = \dot{M}t/at = \dot{M}/a$. The assumption of constant T simplifies the problem greatly, since this leads to $dE/dt = (\partial E/\partial T)\, dT/dt = 0$.

Energy Equation of State

Assume for simplicity that the vapor originated from a monatomic gas of ionization energies ε_j ($j = 1$ to Z). The energy equation of state can then be written as

$$E = \left[\frac{3}{2}T(1 + Z) + \sum_{j=1}^{Z}\varepsilon_j\right]\Big/\mu \qquad (3)$$

where T is in units of energy, and Z is a function of ρ and T. The first term in Eq. (3) represents the kinetic energy of the electrons and ions, while the sum represents the energy required to remove Z electrons from the vapor atoms. The vapor is assumed to be ionized up to charge Z, which may be considered as a continuous variable. We have derived analytical expressions for E in the case of pure carbon and pure aluminum plasmas. To do this, one must calculate Z as a function of ρ and T. The degree of ionization of the vapor can be obtained by solving the Saha equation for each ionized species j, i.e.

$$n_e \frac{n_{j+1}}{n_j} = KT^{3/2}\frac{g_{j+1}}{g_j}\exp\,-\,(\varepsilon_{j+1}/T) \qquad (4)$$

where $K = 6.04 \times 10^{21}$ cm^{-3} eV$^{-3/2}$, subject to the constraints of conservation of heavy species $\rho/\mu = \Sigma_j n_j$, and conservation of charge $n_e = \Sigma_j n_j$. The values of ε_j and g_j for C and Al are given in Table 1.

We have used an iterative procedure to solve the set of equations such as (4) which is based on the fact that at a given ρ and T there will be two dominant ionic species of charge j

and $j + 1$. In order to determine j, we calculate, for a given ρ, a set of θ_j ($j = 1, 2, \ldots$) for which $n_j = n_{j+1} = \frac{1}{2}(\rho/\mu)$. We find from Eq. (4) that θ_j is a solution of the following equation:

$$K\theta_j^{3/2} \frac{g_{j+1}}{g_j} \exp(-\varepsilon_{j+1}/\theta_j) = \frac{2j+1}{2} \frac{\rho}{\mu} \tag{5}$$

Therefore, if T is in the range $(\theta_{j-1} + \theta_j)/2 < T < (\theta_j + \theta_{j+1})/2$, we consider that the two species of charge j and $j + 1$ will dominate. We can then combine Eq. (4) with the equation of conservation of charge

$$n_e = jn_j + (j+1)n_{j+1} \tag{6}$$

and with the equation for conservation of heavy ions

$$n_j + n_{j+1} = (\rho/\mu) \tag{7}$$

to eliminate n_e and n_{j+1} from Eq. (4), thereby obtaining a quadratic equation for n_j, from which we choose the physically acceptable root. The concentrations of minor ionic species are then calculated from the other Saha equations. We have written a simple computer code that solves the set of Saha equations following the procedure outlined above in an iterative way in order to correct the solution of Eq. (4) for the presence of minor species. One finds, to a very good approximation, that Z is given by

$$Z = F + D_1 /// \left\{ \frac{T}{[D_2 + D_3 \log_{10}(\rho/\rho_0)]} \right\} \tag{8}$$

where the F, D_1, D_2, and D_3 are shown in Table 2.

Figures 3 and 4 show a comparison between the "exact" calculation of Z using the equilibrium code and the curve fit given by Eq. (8). The plateau in the ionization level given by $Z(=F) = 3$ for Al and 4 for C corresponds to an ionized plasma where the main ions (C^{4+} and Al^{3+}) have a closed shell of electrons, resulting in a sharp increase in ionization energy as compared to the lower charged ions.

The plateau is delimited by the two temperatures $T_1(\rho)$ and $T_2(\rho)$. T_1 and T_2 can be readily calculated from Eq. (8) by setting $Z = 3$ (aluminum) or 4 (carbon). One sees from Fig. 3 that T_2 for C is sufficiently high that, for our purposes, we need only consider the domains $T < T_1$ (where Z increases with T), and $T_1 < T < T_2$ where $Z(=F) = 4$. Therefore, Table 2 has only two columns of coefficients for C, while three columns are necessary to describe the properties of Al plasmas.

Table 1 Ionization energies and degeneracies of carbon and aluminum ions

Species	ε_j, eV	Degeneracy of ground state, g	Species	ε_j, eV	Degeneracy of ground state, g
Al	6.0	6	C	11.26	9
Al^+	18.8	1	C^+	24.4	6
Al^{2+}	28.4	2	C^{2+}	47.9	1
Al^{3+}	119.6	1	C^{3+}	64.5	2
Al^{4+}	154.0	6	C^{4+}	392.0	1
Al^{5+}	190.0	9	——	——	——

An analytic expression for the energy Eq. (3) can readily be obtained by noting that to a very good approximation, in the region $T < T_1$, we can write for both Al and C

$$\varepsilon_j = Aj + B \tag{9a}$$

so that, upon summation over j

$$\mu E = \tfrac{3}{2}T(1+Z) + Z[(A/2)(Z+1) + B] \tag{10a}$$

We also can write for aluminum, when $Z > 3$ ($T > T_2$)

$$\varepsilon_j = A'j + B' \tag{9b}$$

so that, upon summation

$$\mu E = \tfrac{3}{2}T(1+Z) + (Z-3)[(A'/2)(Z+3) + B'] + C' \tag{10b}$$

where C' is a constant chosen to match solutions (10a) and (10b) when $Z = 3$. The constants entering into Eq. (10) in units of eV/atom are shown in Table 2.

The combination of Eqs. (8) and (10) results in an analytic approximation for the energy equation of state $E(\rho, t)$ of the plasma. We show in Figs. 5 and 6 a comparison between the analytic approximation and the more exact results using the ionic concentrations given by the equilibrium code. The fit is seen to be quite good over the range of temperatures and densities considered.

Graphical Solution of Coupling Equations

Once ε and E have been determined, one can readily solve the coupled Eqs. (1) and (2) by graphical means. A graphical solution, using the energy equation derived above, is shown in Figs. 7 and 8. Figure 7a shows the relationship between incident intensity and temperature in slab II. These curves were obtained by equating $2\varepsilon\sigma T^4$ with I, which is equivalent to the requirement that slab II reradiate all the energy absorbed from the laser beam and not heat up (i.e., $dT/dt = 0$). Figure 7b, for aluminum, and Fig. 8, for carbon, show plots of constant $\dot{M}$ and constant I, generated on a programmable hand calculator, as a function of ρ and T. The plots $\dot{M}$ = const were obtained by writing

$$\dot{M} = \rho a = (\rho/\rho_0)\rho_0[\gamma k_B T(1+Z)/\mu]^{1/2} \tag{11}$$

The plots I = const were obtained by solving Eq. (1) with $\varepsilon\sigma T^4$ replaced by $I/2$, i.e.

$$\rho/\rho_0 = \frac{I/2}{\rho_0 a(H_v + E + a^2/2)} \tag{12}$$

Equation (12) is an implicit equation for ρ/ρ_0 as a function of T, for I given. The graphical solution is as follows. Let the

Table 2 Constants in Eqs. (4) and (7)

Temperature range	Carbon		Aluminum		
	$T < T_1$	$T > T_1$	$T < T_1$	$T_1 < T < T_2$	$T > T_2$
D_1	2.4	0	1.3	0	3.56
D_2	2.29	——	0.8	——	4.82
D_3	0.85	——	0.15	——	0.74
F	0	4	0	3	0
$A(A')$	17.5	17.5	11.5	11.5	35.5
$B(B')$	−5.8	−5.8	−5.5	−5.5	−23
C'	——	——	——	——	52.5

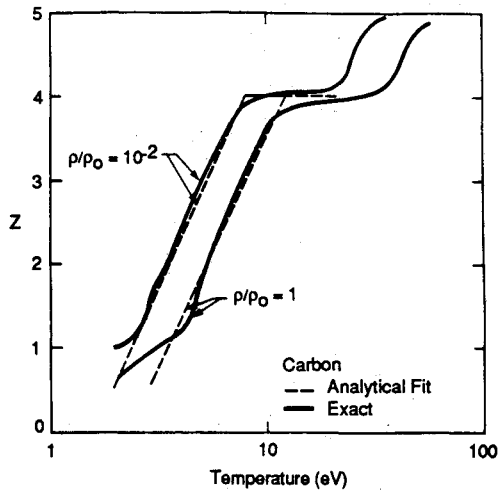

Fig. 3 Degree of ionization of carbon.

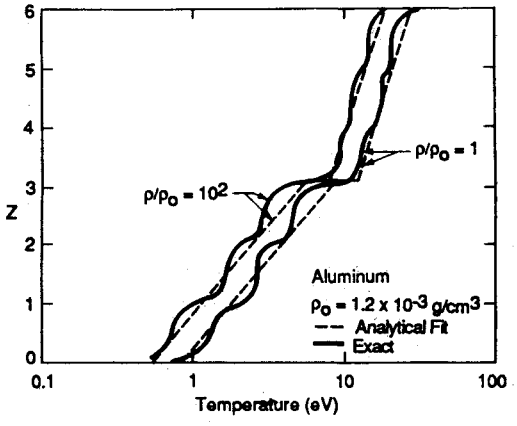

Fig. 4 Degree of ionization of aluminum.

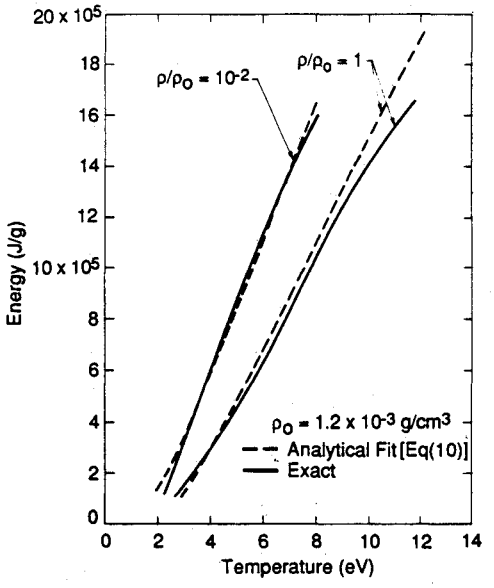

Fig. 5 Energy per unit mass of carbon vapor.

laser intensity be given. Then, from Fig. 7a, if we know the slab emissivity ε, we can obtain from the corresponding curve the T of slab II. T and I then determine in Fig. 7b the value of ρ/ρ_0. The $\dot{M}$ = const curve passing through the point $(\rho/\rho_0, T)$ yields $\dot{M}$. The total mass per unit area of vapor, assuming $\dot{M}$ to be constant, is $\dot{M}t$. $\dot{M}$ vs I for aluminum and carbon is shown in Fig. 9, with the assumption $\varepsilon = 0.5$. The blowing rate in aluminum is seen to be 2–4 times larger than

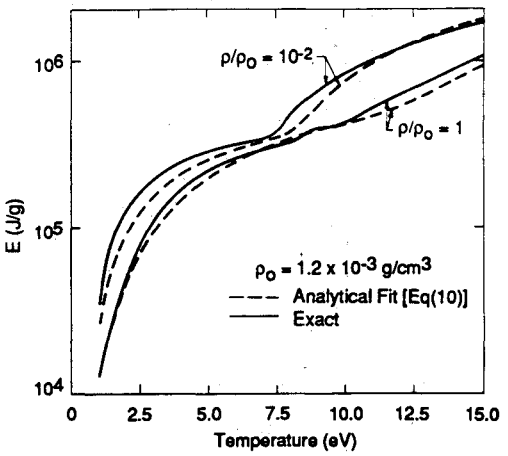

Fig. 6 Energy per unit mass of aluminum vapor.

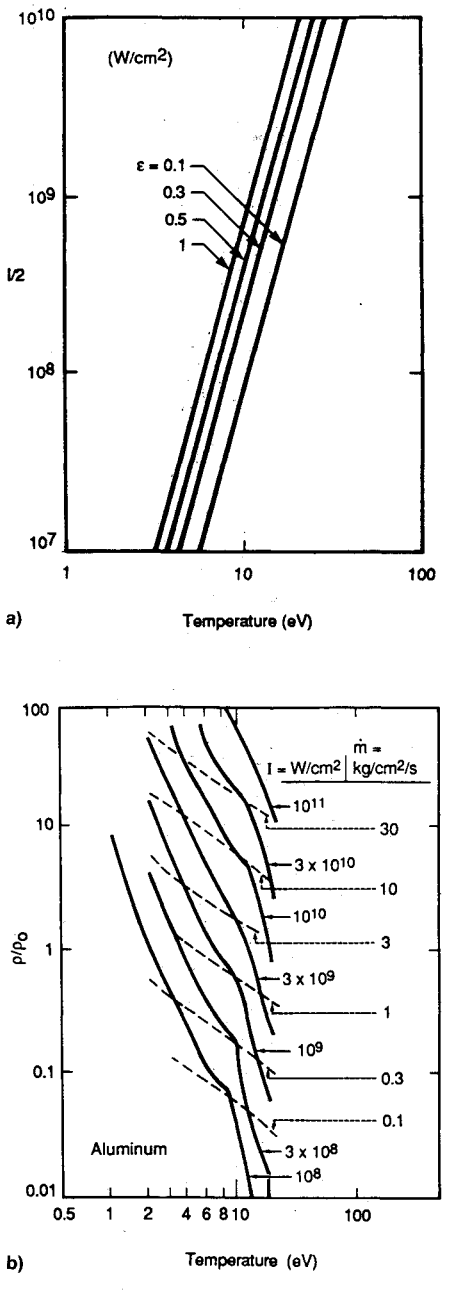

Fig. 7 Graphical solution to mass removal equations for aluminum: a) $I/2$ vs T for different slab emissivities and b) curves of constant $\dot{M}$ and I vs plasma properties.

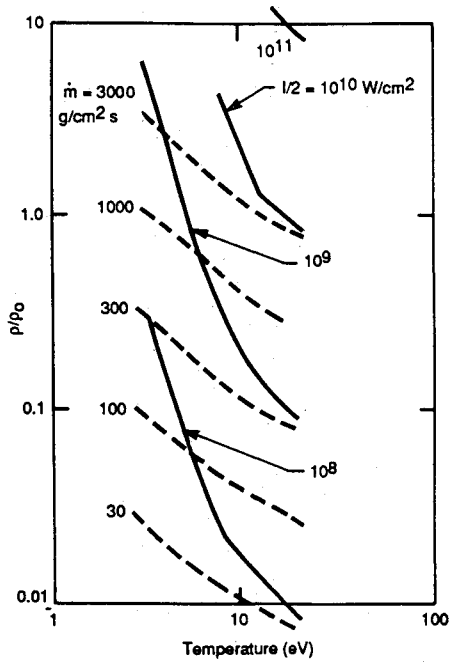

Fig. 8 Curves of constant $\dot{M}$ and I vs plasma properties, carbon.

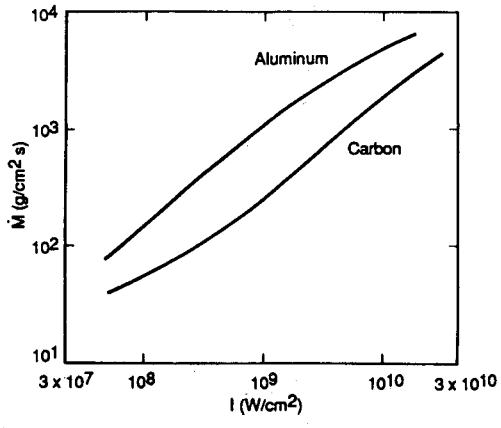

Fig. 9 Mass loss rate in carbon and aluminum for $\varepsilon = 0.5$.

that in carbon for the range of intensities considered. One has the approximate scaling $\dot{M} \propto I^{2/3}$.

A determination of the ε of the plasma requires a knowledge of the radiative properties of the ionized species involved and a knowledge of the plasma thickness. The bulk of the plasma expands at the sound velocity so that it is a good approximation to write

$$L = a(\rho, T)t \tag{13}$$

with a given by Eq. (11).

Extensive calculations of radiative properties of plasmas composed of atomic species of nuclear charge less than 30 have been carried out at the Los Alamos National Laboratory,[8,9] and are presently being updated to include higher nuclear charge species up to neon.[10] A similar effort has been carried out at Lawrence Livermore Laboratory.[11] The data presented are in the form of tables of Rosseland opacities at various values of T and ρ for a set of plasma compositions. Since we need, for our purposes, to calculate slab emissivities rather than Rosseland opacities, we have used a radiation code that was developed many years ago at Physical Sciences Inc.[12]

Aluminum slab emissivities as a function of T for several values of L and (ρ/ρ_0) are shown in Fig. 10. The radiation code that we used includes radiation from free-free (bremsstrahlung), free-bound (photorecombination), and bound-bound electron transitions in the plasma. Transitions for ions up to charge $Z = 6$ were included in our calculations. Line intensities were taken from the tabulations of Wiese,[13] Stark broadening parameters for the calculation of line widths were taken from Griem.[14] The photoionization cross sections that we used for the ground states of Al and C were taken from Refs. 15 and 16, respectively. Other photoionization cross sections for ground and excited states were calculated by using a hydrogenic approximation to these states. A discussion of the formulas used in the code can be found in Ref. 12. The emissivities thus calculated are in very good agreement with the results of Romanov et al.,[17] as shown in Fig. 11.

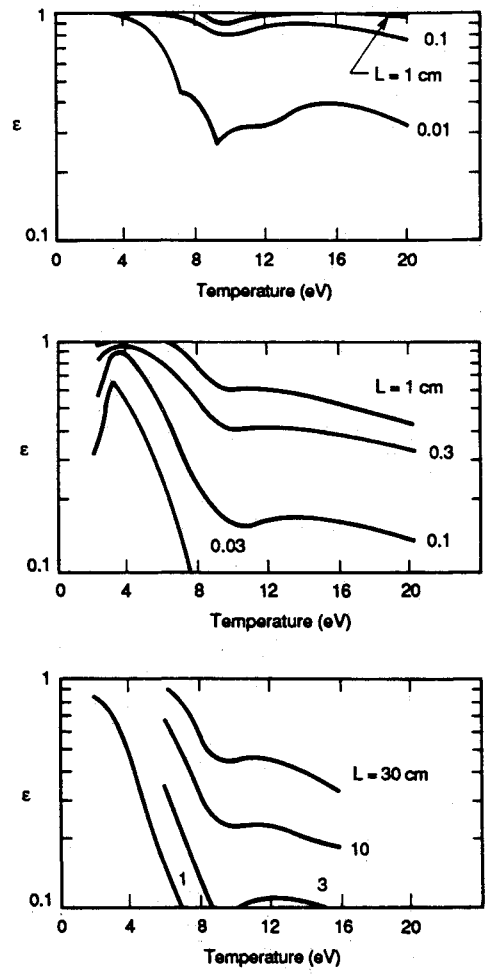

Fig. 10 Aluminum slab emissivities: a) $\rho/\rho_0 = 10$, b) $\rho/\rho_0 = 1$, and c) $\rho/\rho = 0.1$.

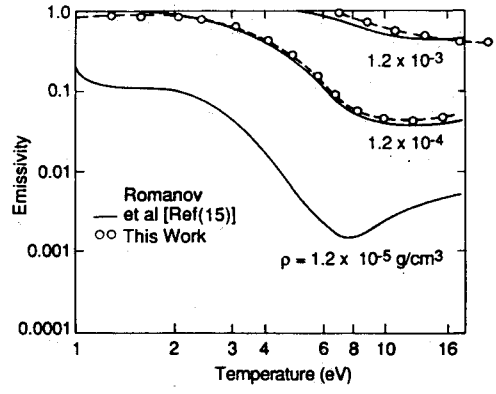

Fig. 11 Emissivity of a 1-cm aluminum slab.

The graphical solution discussed above requires a knowledge of ε. An iterative procedure should be used in which, for the initial iteration, an educated guess for ε is made. A

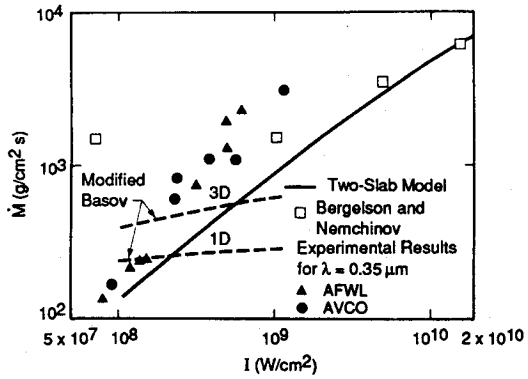

Fig. 12 Mass loss rate from aluminum surface.

first solution then yields T and (ρ/ρ_0). This yields $\dot{M}$ and $a(\rho, T)(=\dot{M}/\rho)$ from Fig. 8. Since the slab thickness by the end of the pulse is at_p, the actual slab emissivity can then be obtained from interpolation of the results in Fig. 10. We have used this procedure to compare our results with experimental values[18] and with the numerical results of Bergelson and Nemchinov.[7] The comparison is shown in Fig. 12. Agreement with the results of Bergelson and Nemchinov,[7] where they considered an aluminum surface irradiated by a blackbody at 5, 10, 15, and 20 eV, respectively, is seen to be excellent except at the lowest flux, $I = 7 \times 10^7$ W/cm^2 (corresponding to $T =$ 5 eV). The experimental data was taken by two groups using an XeF laser ($\lambda = 0.35$ μm) at AVCO that delivered ~400 J in 1.3–1.6 μs. The intensity was varied by changing the beam radius at the surface from $R = 1$ cm at $I = 10^8$ W/cm^2 to $R = 0.3$ cm at $I = 10^9$ W/cm^2. Using the results from the two-slab model we calculated that $L = 1.2$ cm ($a = 10^6$ cm s^{-1}) and 1.7 cm ($a = 1.3 \times 10^6$ cm s^{-1}) at $I = 10^8$ and 10^9 W/cm^2, respectively. The ratio L/R increases from a value of 1 to a value of 5.5 as the laser intensity is increased from 10^8 to 10^9 W/cm^2. Thus, at laser intensities above 10^8 W/cm^2, the flow cannot be considered as one-dimensional. The radial acoustic relaxation time at the highest flux density used in the experiments $R/a = (0.3 \text{ cm})/(1.3 \text{ cm s}^{-1}) = 0.2$ μs, and the flow can only be treated as one-dimensional up to this time. In spite of the three-dimensional nature of the flow for $I >$ 10^8 W/cm^2, the two-slab model of the interaction gives mass loss rates that are only a factor of 3 lower than the measured rates at laser intensities below 10^9 W/cm^2.

It is of interest to compare our results with the results derived from the Basov theory,[3] i.e., with the neglect of radiative effects. We have modified the Basov treatment in order to take into account the energy expended in multiply ionizing the vapor (which was not included in the derivation of the scaling relations). We use for electron-ion inverse bremsstrahlung absorption coefficient

$$k = 3.69 \times 10^8 \bar{G} \frac{Z^2}{T^{1/2}\nu^3} n_i n_e \{1 - \exp[-(h\nu/k_B T)]\} \text{ (cm}^{-1}\text{)} \tag{14}$$

where ν is the laser frequency, T is in Kelvin, and $\bar{G}$ is a Gaunt factor of order unity that we set equal to 1.3 for our range of operating conditions.[19] Equation (14), which was taken from Ref. 20 with the addition of the Gaunt factor and of a factor to take into account stimulated emission, can be recast in terms of ρ, since $n_i = Zn_e = \rho/\mu$. We obtain the following result for Al, under the conditions $h\nu/k_B T \ll 1$ and $\lambda = 0.35$ μm:

$$k = 1.24 \times 10^7 (Z^3\rho^2/T^{3/2}) \text{ (cm}^{-1}\text{)} \tag{15}$$

where ρ is in g/cm^3, and T in eV. Note that the prefactor in Eq. (10) scales as λ^2.

The one-dimensional Basov model assumes that $kL = kat_p = 1$. When we combine this with the conservation of energy equation $\dot{M}(\varepsilon + a^2/2) = I$, where $\dot{M} = \rho a$, and use our derived expressions for Z and ε as a function of ρ and T, we can readily calculate ρ and I as a function of T. To do this we fix T and calculate k by varying ρ until the condition $kL = 1$ is satisfied. Since Z depends weakly on ρ, and consequently, a is also weakly dependent on ρ, kL will be proportional to ρ^2. An iteration over ρ will lead to rapid convergence. With ρ and T known, then I can be obtained from the conservation of energy equation. The resulting $\dot{M}$ vs I is shown in Fig. 12. Since for $I > 10^8$ W/cm^2, the expansion is three dimensional, we must also compare the experimental results with the three-dimensional Basov model[3] where the condition $kL = 1$ is replaced by $kR = 1$, and the specific energy ε in the conservation of energy equation is replaced by the specific enthalpy, so that we must add to ε the term $k_B T(1 + Z)/\mu$. The results for the three-dimensional model are also shown in Fig. 12. One sees that for both models $\dot{M}$ is rather insensitive to I. Both models significantly underpredict the values of $\dot{M}$ at the larger laser intensities. One must also note that the mass loss rates in both Basov models are sensitive to λ ($\dot{M}$ would be a factor of roughly 3 lower if we had used $\lambda = 1$ μm instead of 0.35 μm), while the two slab model results are independent of λ.

The larger than predicted values of $\dot{M}$ observed at high laser fluxes are believed to be due to three-dimensional edge effects. There are three effects that can lead to enhanced coupling. Firstly, due to the lateral expansion of the plasma, the plasma will have enhanced transparency to the laser beam near the beam edge. Secondly, the plasma radiation in the three-dimensional regime will affect a larger radius of the target as the plasma moves further away from the surface. And lastly, the plasma, having a negative index of refraction, will act as a diverging lens, leading to irradiation of the target outside the normal beam. The lateral deflection distance at the surface scales as $(n_e/n_{ec})L^2/R$, where n_{ec} is the critical electron density ($n_{ec} = 10^{22}$ cm^{-3} at $\lambda = 0.35$ μm). We estimate this deflection to be of the order of 1 mm for the measurements carried out at 10^9 W/cm^2. All three effects will lead to enhanced vapor formation near and beyond the edge of the beam.

Discussion

The two-slab model for plasma mediated coupling, as shown in this article, gives mass loss rates that are in reasonable agreement with experiments and that do not differ appreciably from a much more detailed and complex model[4] of the interaction. The domain of validity of the model is, however, restricted. It is not applicable to the transient conditions, corresponding to short pulse times and/or low intensities when a plasma has not been formed or has not reached steady state. We neglected in the energy equation the energy of slab I as compared to slab II. Slab II must have a sufficient mass so that the energy stored in it is much larger than that of slab I. It must also have an emissivity of near unity. The above requirements place a lower limit on the laser pulse length. If the length and mass of slab II are so large that $L/l_R \gg 1$, then the assumption of constant T within the slab will be poor.

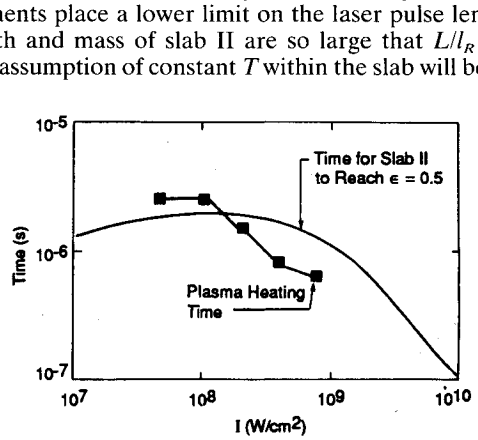

Fig. 13 Minimum pulse time for two-slab model to apply.

Therefore, there will be an upper limit to t_p for which the model applies. We show in Fig. 13 the minimum t_p required for slab II to have an emissivity = 0.5. The transient times for plasma mediated coupling in aluminum can be inferred from Fig. 1. If we define the transient time as being the time at which the (peak) temperature in slab II has reached 90% of its asymptotic value, we obtain the squares in Fig. 13. We see from this figure that both times are comparable to within a factor of 2. The time for ε to reach a value of 0.5 is seen to remain practically constant ($t_p \simeq 1-2 \times 10^{-6}$ s) up to $I \simeq 10^9$ W/cm^2, and then drop as I^{-1}. The constant value is associated with the sharp drop in plasma opacity, shown in Fig. 10, as the aluminum temperature increases from 4 to 8 eV. Thus, even though $\dot{M}$ increases with I, the total mass $M = \dot{M}t_p$ required for $\varepsilon = 0.5$ also increases, resulting in $t_p \simeq$ const ($\simeq 10^{-6}$ s). The experimental results shown in Fig. 12, corresponding to $1.3 < t_p < 1.6$ μs, just barely fall in the region where our steady-state, two-slab model is applicable.

The constant T approximation for slab II will be a poor approximation for long laser wavelength ($\lambda >> 1$ μm) as shown in the numerical results of Bergelson and Nemchinov.[4] The absorption length in the plasma at large λ will be so short that slab II will have a large temperature gradient. This would result in an overestimate of $\dot{M}$ if one were to use the predictions of the two-slab model.

One can deduce from the physical assumptions underlying the model how $\dot{M}$ will scale with gas properties. Since $\varepsilon\sigma T^4 = I/2$, we see that $T = A(I/\sigma)^{1/4}$, where the factor A, which is close to unity, depends weakly on gas properties and pulse duration. Therefore, from Eq. (16)

$$\dot{M} = \rho C_s = \frac{I/2}{H_v + E + a^2/2} \simeq \frac{I/2}{E(T)} \qquad (16)$$

The blowing rate will scale inversely with $E(T)$, T being nearly equal to $(I/\sigma)^{1/4}$. As an example, for $I = 10^9$ W/cm^2 we have $T = 9$ eV and $E(9\text{ eV}) = 1.3 \times 10^6$ J/g for carbon, and 4.3×10^5 J/g for aluminum (for $\rho/\rho_0 = 1$). One would therefore expect that $\dot{M}(\text{C}) \simeq 0.3\dot{M}(\text{Al})$ which is close to the ratio of calculated $\dot{M}$ (see Fig. 1).

The model that we developed is only valid for a one-dimensional interaction. Radial effects will come into play when the interaction is affected by 1) lateral expansion of the plasma and 2) lateral radiative losses. For both of these effects to be negligible, one must have $L < R$, or $T_p << R/(C_s L)$.

Acknowledgment

This work was funded by the Defense Nuclear Agency, Alexandria, Virginia, under Contract DNA-001-83-C-0186.

References

[1]Grey Morgan, C., "Laser-Induced Breakdown of Gases," *Reports on Progress in Physics*, Vol. 38, No. 5, 1975, pp. 621–665.

[2]Weyl, G. M., "Physics of Laser-Induced Breakdown: An Update," *Laser-Induced Plasmas and Applications*, edited by L. Radziemski and D. Cremers, Marcel Dekker, New York, 1989, Chap. 1, pp. 1–67.

[3]Basov, M., Gribkov, V., Krokhin, A., and Slizkov, G., "High Temperature Effects of Intense Laser Focused on a Target," *Soviet Physics—JETP* (translation of *Zhurnal Eksperimental'noi i Teoretischeskoi Fiziki*), Vol. 27, No. 4, 1968, pp. 572–582.

[4]Bergelson, V., and Nemchinov, I., "Parameters of a Plasma Formed by the Action of Microsecond Laser Pulses on an Aluminum Target in Vacuum," *Soviet Journal of Quantum Electronics* [translation of *Kvantovaya Elektronika* (Moscow)], Vol. 8, No. 10, 1978, pp. 1198–1202.

[5]Bergelson, V. I., and Nemchinov, I. V., "Numerical Investigation of Laser Interaction with a Target in Vacuum, Including the Spectral Composition of the Radiation Emitted by the Generated Plasma," *Soviet Journal of Quantum Electronics* [translation of *Kvantovaya Elektronika* (Moscow)], Vol. 10, No. 11, 1980, pp. 1373–1375.

[6]Shui, V., Kivel, B., and Weyl, G., "Effect of Vapor Plasma on the Coupling of Laser Radiation with Aluminum Targets," *Journal of Quantitative Spectroscopy and Radiative Transfer*, Vol. 20, No. 11, 1978, pp. 627–636.

[7]Bergelson, V., and Nemchinov, I., "Heating of an Expanding Plasma by Continuum Radiation," *Soviet Journal of Plasma Physics* (translation of *Fizika Plazmy*), Vol. 7, No. 11, 1981, pp. 184–189.

[8]Huebner, W. F., Merts, A. L., Magee, N. H., and Argo, M. F., "Astrophysical Opacity Library," Los Alamos National Lab., LASL 6760-M, Los Alamos, NM, 1977.

[9]Weiss, A., Keady, J. J., and Magee, N. H., "A Collection of Los Alamos Opacity Tables for All Temperatures," *Atomic Data Nuclear Data*, Vol. 45, No. 2, 1990, pp. 209–238.

[10]Magee, N. H., private communication, Los Alamos National Lab., Los Alamos, NM, 1992.

[11]Rogers, F. J., and Iglesias, C. I., "Radiative Atomic Rosseland Mean Opacities," *Astrophysical Journal Supplement*, Vol. 79, No. 2, 1992, pp. 507–568.

[12]Pirri, A. N., and Root, R. G., "Theoretical Analysis of Radiation from Laser Produced Plasmas," AIAA Paper 79-1489, July 1979.

[13]Wiese, W., Smith, M., and Miles, B., *Atomic Transitions Probabilities, Vol. II, Sodium Through Calcium*, U.S. Government Printing Office, NSRDS-NBS 22, Washington, DC, 1969.

[14]Griem, H., *Plasma Spectroscopy*, McGraw-Hill, New York, 1964.

[15]Hudson, R. D., and Kieffer, L. J., "Compilation of Ultraviolet Photoabsorption Cross Sections for Atoms Between 5 and 3000Å," *Atomic Data*, Vol. 2, 1977, pp. 205–262.

[16]Magee, N. H., Merts, A. L., and Huebner, W. F., "Is the Metal Contribution to the Astrophysical Opacity Incorrect?," *Astrophysical Journal*, Vol. 283, No. 2, 1984, pp. 264–272.

[17]Romanov, G. S., Stepanov, K. L., and Syrkin, M. I., "Optical Properties of a High-Temperature Aluminum Plasma," *Optics and Spectroscopy* (USSR), Vol. 53, No. 4, 1982, pp. 381–384; *Optika i Spektroskopyia*, Vol. 53, 1982, pp. 642–648.

[18]Duzy, C., private communications, 1986.

[19]Karzas, W. J., and Latter, R., "Electron Radiative Transitions in a Coulomb Field," *Astrophysical Journal Supplement*, Vol. 6, No. 5, 1961, pp. 167–221.

[20]Zel'dovich, Ya. B., and Raizer, Yu. P., *Physics of Shock Waves and High Temperature Hydrodynamic Phenomena*, Vol. 1, Academic Press, New York, 1966, p. 259.